Proceedings of the ASME 2011 5th International Conference on Energy Sustainability
ES2011
August 7-10, 2011, Washington, DC, USA

ES2011-54202

Analysis of Performance of Direct Dry Cooling for Organic Rankine Cycle Systems

Daniel Zimmerle
Engines and Energy Conversion Laboratory,
Mechanical Engineering Department,
Colorado State University,
Fort Collins, CO, USA

Nicholas Cirincione
Engines and Energy Conversion Laboratory,
Mechanical Engineering Department,
Colorado State University,
Fort Collins, CO, USA

ABSTRACT

The performance of dry-cooled ORC systems varies significantly with environmental conditions, diurnally and seasonally. This study analyzes the impact of environmental conditions on overall performance and operational control of dry-cooled ORC systems with fixed and variable geometry expanders. Performance analysis results are extended to time-series environmental data to determine the expected performance of a system over long durations. Analysis results indicate that, if other factors are held constant, variable speed condenser fans produce minimal performance improvement, while variable-geometry expanders have a significant impact.

NOMENCLATURE

ORC – Organic Rankine Cycle
ICE – Internal Combustion Engine
EECL – Engines and Energy Conversion Laboratory
CSU – Colorado State University
SRRL – Solar Radiation Research Laboratory, Golden, CO, USA

Operators:

Δ	change

Variables:

h	enthalpy, (KJ/Kg)
P	pressure, (Pa)
s	entropy, (J/K)
H	heat transfer coefficient
$\dot{m}$	mass flow rate (kg/s)
$Q, \dot{Q}$	heat transfer (KJ), heat transfer rate (KW)
T	air temperature, (°C, K)
$W, \dot{W}$	work (KJ), work rate (KW)
N	fan speed
η	efficiency, unitless
τ	working fluid temperature (°C, K)
C_p	specific heat

Subscripts and superscripts

p	pump
b	boiler
e	expander
c	condenser, condenser conditions
i	inlet
o	outlet
a	air
f	working fluid
n	nominal, or design conditions
min	minimum
max	maximum allowed
1,2,..5	Numerical subscripts refer to states in Figure 1.

1. INTRODUCTION

In 2005 it was estimated Organic Rankine Cycles (ORCs) could be used to generate as much as 750 MW of energy in the United States [1]. Much of the heat used to drive those ORCs comes from low grade (90-250 °C) sources such as low-magnification solar concentrators, geothermal, internal combustion engines (ICEs) and ocean thermal energy

conversion [2-8]. Generally, ORCs are most profitable when used with waste heat sources that exhibit high availability, producing consistent waste heat flows for extended periods. Ideal sources with high availability include dedicated sources such as geothermal or low-temperature solar concentrators, high-utilization secondary applications, such as industrial processes, or high-utilization transportation or electrical generation sources, such as locomotives, marine vessels, and gas compressor stations.

While Rankine cycles have been utilized since the early industrial revolution, recent developments in organic working fluids make possible cycles that operate safely at lower temperatures. These new hydrofluorocarbon (HFC) working fluids are ozone-safe, although there are some concerns about their green-house gas equivalence [9]

All Rankine cycle processes require a cooling source to condense the working fluid at the low working temperature. Design of acceptable condensers poses significant challenges. Currently, most low-temperature ORC systems utilize evaporative cooling systems. However, water consumption in evaporative cooling is problematic in arid regions, including the western United States, where water resources are scarce [10]. An alternative is to utilize "dry cooling" – cooling using only moving airflow, typically using fin & tube heat exchangers with forced-air flow. Dry coolers can range dramatically in size, from automotive radiators to large industrial fin-fan coolers.

Dry cooling may be implemented in two methods. First, the dry cooler can be utilized to cool a secondary water loop, which is then utilized to condense the ORC working fluid. An advantage of this method is to reduce the amount of working fluid, since water, not working fluid, is routed through the dry cooler – typically a significant system volume. However, this method requires two heat exchange steps, with associated pumping loads and pinch points. For low-temperature sources, such as ICE jacket water or many geothermal sites, the combined pinch point raises the ORC bottom temperature, reducing the cycle efficiency to an unacceptable level. As a result, there has been increasing interest in the second method: Directly condensing the ORC working fluid in the dry cooler. This method reduces the pinch point penalty at the cost of increased working fluid mass and increased variability in changing ambient conditions.

Traditional thermodynamic studies attempt to identify the optimum system configuration for selected environmental conditions and system constraints [11-15]. Any ORC can be optimized only for one pair of boiler and condenser temperatures. Other studies [16-18] do account for a varying condensing temperature, but not as it applies to overall efficiency over an extended time period. This study extends traditional analysis to consider the operation of a system *after* it has been designed and built. Evaporative cooling allows some manipulation of the condenser temperature independent of the ambient temperature by varying water flow into the cooling tower. However, in the case of dry cooling, control of condenser temperature is much more difficult. Variable-speed fans provide some control of condensation temperature, but generally, the cycle must operate over a wider range of condenser temperatures than an evaporatively cooled system.

Finally, most waste heat cycles are coupled to a finite heat source. At cold ambient temperatures, when the cycle temperature delta and efficiency increase, the flow rate of working fluid through the ORC system is capped by the availability of waste heat. At hot ambient temperatures, the cycle temperature delta and efficiency decrease, and other system components, such as the condenser or expander, will determine the mass flow through the ORC system.

This system analysis is based upon an existing ORC research system at Colorado State University's (CSU) *Engines and Energy Conversion Laboratory* (EECL). The cycle is designed to utilize jacket cooling water from large ICEs as the waste heat source. While the cycle could operate utilizing a number of working fluids, R245fa was selected for both the analysis and the system. R245fa (1,1,1,3,3 pentaflouropropane) possesses several properties that make it attractive for low-temperature ORC systems, including a low boiling point and low operational pressures, which reduce overall system cost. The system was designed to operate successfully at 30 °C. This analysis considers operation over a temperature range of -35 to +40 °C, utilizing the same equipment. The study considers the advantages of variable-speed fans on the condenser, and also compares two expander types – a fixed-nozzle turbine and a hypothetical positive-displacement expander. Temperature data for three years, taken from the Solar Radiation Research Laboratory (SRRL) in Golden, Colorado, are utilized for comparing overall system performance in the different configurations.

This paper first describes the system and system modeling methodology, including methods for computationally balancing the cycle. Results are then presented for several system configurations, comparing variable- and fixed-speed fans, and two expander configurations. Finally, results and conclusions are presented.

2. SYSTEM MODELING

2.1 OVERVIEW

Figure 1 provides a schematic of the system. Circled numbers indicate the five independent thermodynamic states in the system. The system is driven by a 250 KW water waste heat stream at 93 °C, part of the cooling water jacket flow from a 1.8 MW ICE. The boiler supports a tight pinch point of 5 °C, allowing the boiler to produce saturated vapor at 88 °C, with the potential of a maximum of 5 °C of superheat. The system was designed to utilize 250 KW of waste heat at an ambient temperature of 30 °C. The site is at an elevation of 1524 m, and exhibits a standard air pressure of approximately 84 KPa. While electrical components are shown in the figure for clarity, these were not considered in the analysis.

Variability is imposed upon the system by changes in ambient temperature and humidity which affect the cycle through the air-cooled condenser. Control is provided through two mechanisms. First, a variable speed drive controls pump

speed, which, when coupled with the flow resistance in the turbine nozzles and control valve, controls the working fluid flow rate, $\dot{m}_f$. Second, for modeling purposes, variable speed fans are assumed to control condenser air flow rate, $\dot{m}_a$. The actual system is equipped with fixed-speed fans. The amount of heat available and heat input temperature are held constant for all simulations.

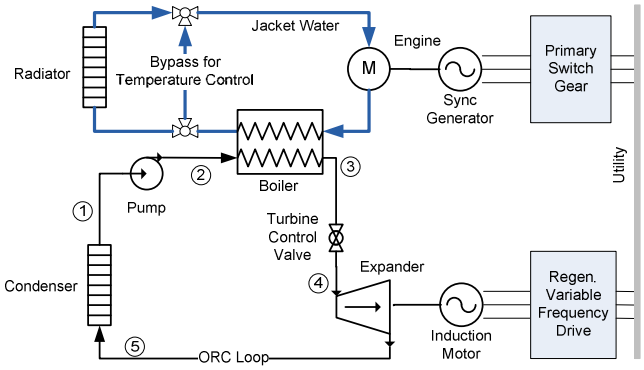

Figure 1: System Overview

2.2 EQUIPMENT MODELS

Pump: The system utilizes a sliding vane, positive displacement pump. This type of pump exhibits nearly constant efficiencies across a wide range of flow rates and pressure differentials, and was modeled as isentropic compression at a constant efficiency. The change in enthalpy due to pumping work is calculated as a function of the boiler pressure and the efficiency of the pump.

$$\Delta h_p = \frac{h_2^*(P_2, s_1) - h_1}{\eta_p} \quad (1)$$

Where $h_2^*(P_1, s_1)$ indicates enthalpy as an isentropic transition from state 1 to pressure 2. Pump power is then:

$$\dot{W}_p = \dot{m}_f * \Delta h_p \quad (2)$$

The pump's output pressure is set as the saturation pressure at the boiler temperature. Since the waste heat is constant, the boiler temperature and pressure are also constant for all simulations.

Boiler: The boiler vaporizes the working fluid at a fixed pressure to saturation, and is modeled as direct heat addition with no pressure drop. At mass flow rates significantly below the design flow rate, the working fluid will be slightly superheated. However, since maximum superheat is limited by the waste heat temperature to 5 °C, this effect was neglected.

Flow through the boiler is limited by the available waste heat. Since the total power transferred in the boiler is:

$$\dot{Q}_b = \dot{m}_f \Delta h_b \quad (3)$$

the mass flow rate is limited to:

$$\dot{m}_f = \frac{\dot{Q}_b}{\Delta h_b} : 0 < \dot{m}_f < \frac{\dot{Q}_{max}}{\Delta h_b} \quad (4)$$

where $\dot{Q}_{max}$ is the maximum allowable waste heat rate, or 250 KW.

Expander and Control Valve: The current expander is an experimental Tesla turbine primarily designed as a replacement for steam expansion valves in industrial processes. It has fixed nozzle geometry, which sets the mass flow rate as a function of the pressure differential across the turbine, i.e. $\dot{m}_f = \mathcal{F}(\Delta P_e)$. Given the available data, efficiency was modeled as a function of mass flow rate, i.e. $\eta_e = \mathcal{F}(\dot{m}_f)$. Currently, no experimental data exists for R245fa as a working fluid. However, it is expected that the expander's performance, tuned for R245fa, will closely resemble its behavior for steam, for which test data exists. To model the turbine, existing experimental data was normalized to design conditions, quadratic curves were fit to the data, and these curves utilized in the model. The expander exhibits a maximum efficiency of 57% at its design mass flow rate – a performance in line with similarly sized devices reviewed by the authors. The mass flow rate is an only slightly non-linear function of the pressure delta across the turbine.

A fixed-nozzle expander and control valve operate together to set the mass flow rate for the system. With the control valve fully open, flow rate is set by the expander, as indicated above. When ΔP_e exceeds a threshold value, the mass flow through the turbine will exceed the limits set by Eqn 4. The control valve is then partially closed, creating a pressure drop upstream of the turbine, reducing the pressure drop across the turbine, and controlling the total flow rate. Since the valve is small and can be insulated, the pressure drop across the control valve is modeled as an isenthalpic drop. The expander is modeled similarly to the pump, with a variable isentropic efficiency set by the mass flow rate.

In addition to the fixed-nozzle case, the analysis was also extended to a hypothetical expander which can control the mass flow rate independent of the expansion ratio. This behavior is possible with positive displacement expanders that possess both variable geometry and independently controllable inlet valves, or turbines with variable nozzle geometry. In this case, no control valve is required, as the expander itself can control mass flow to any rate, within design limitations. To compare the two types of expanders, the same efficiency relationship was utilized for both expanders.

To distinguish the two types of expanders in this analysis, the fixed-nozzle expander will be referenced as the *fixed* expander, while the infinitely variable expander will be referenced as the *inf* expander.

Condenser: The condenser is a fin-fan dry cooler, similar to an industrial radiator. To speed simulation, several simplifying assumptions were made. The total heat transfer coefficient was computed over a range of conditions using AspenTech's heat exchanger design software, Aspen Exchanger Design & Rating. Mass flow of the working fluid was varied from 0.63 to 1.89 Kg/s, air temperature between -30 and 40 °C, and condenser pressures from 0.2 to 0.65 MPa. Over that range of conditions, the total heat transfer coefficient varied by less that ±5%, and a spot check of simulations indicated that the variation in heat transfer coefficient had minimal impact on the

results. Therefore, the heat transfer coefficient was held constant at the condenser's specification, as $H_c = 22.0\ \frac{W}{m^2 K}$.

Working fluid entering the condenser is somewhat superheated; condensate exiting the condenser is assumed to be at saturation. Since a heat exchange analysis indicated that condensing accounts for the vast majority of heat transfer (approximately 92% at design conditions), all heat exchange was considered to occur between the condensation temperature and the average air temperature. Complete condensation is assumed at all times, setting the heat transfer rate in the condenser to:

$$\dot{Q}_c = \dot{m}_f \Delta h_c \tag{5}$$

which allows computation of the required air mass flow rate as:

$$\dot{m}_a = \frac{\dot{Q}_c}{H_c(\tau_c - \bar{T}_a)} \tag{6}$$

where $\bar{T}_a$ is the average temperature of the air in the condenser, specifically:

$$\bar{T}_a = \frac{1}{2}(T_i + T_o) \tag{7}$$

Assuming constant specific heat for the air at inlet conditions, $\dot{Q}_c$ can also be calculated as:

$$\dot{Q}_c = \dot{m}_a C_{p,a}(T_o - T_i) \tag{8}$$

Combining the last three equations and solving for the condensation temperature as a function of the input air temperature:

$$\tau_c = \dot{Q}\left(\frac{1}{H_c} + \frac{1}{2\dot{m}_a C_{p,a}}\right) + T_i \tag{9}$$

However, since $\dot{Q}$ is a complex function of the condensation temperature and other conditions, the cycle states must be computed iteratively to find the value of τ_c that satisfies both Eqns 5 and 9.

A key analysis optimizes cycle output by varying the condenser fan speed across a range of temperatures. Condenser fan power was modeled using the well known fan laws to scale from design conditions to other operating points. Mass flow scales directly with fan speed, as

$$\frac{\dot{m}_a}{\dot{m}_n} = \frac{N_a}{N_n} \tag{10}$$

Similarly, fan power consumption is given by:

$$\frac{\dot{W}_a}{\dot{W}_n} = \left(\frac{N_a}{N_n}\right)^3 = \left(\frac{\dot{m}_a}{\dot{m}_n}\right)^3 \tag{11}$$

The efficiency of the fan, and its variable speed drive was considered constant for this analysis.

2.3 CLOSING THE CYCLE

To compute the entire cycle, environmental conditions must be specified. Both temperature and relative humidity were considered, but since humidity had negligible impact on the results, only variation in ambient temperature (i.e. T_i) was considered. As indicated above, solution to the cycle equations is inherently iterative. In practice, a condensation temperature is assumed, and all states in the Rankine cycle are computed. States 4 and 5 are then utilized to compute the condensation temperature from Eqn 9, as described above. The unique solution to the cycle is found by reducing the difference between the assumed and computed condenser temperatures to near zero. The *fminbnd()* function in MatLab™ was utilized to perform this minimization, using the built-in golden section search algorithm with a tolerance of 10^{-4}, which does not require the slope of the minimization surface to be calculated.

All fluid and air properties were computed using RefProp™ software from NIST [19].

Since component properties are considered fixed at the design conditions, the key measure of system performance is the net output, defined as:

$$\dot{W}_{out} = \dot{W}_e - \dot{W}_p - \dot{W}_a \tag{12}$$

2.4 SYSTEM MODELING

This analysis considers the performance of a system designed for one ambient temperature, across a range of temperatures. Therefore, the capabilities of all system components are set *a priori*, and the performance of the system is measured using those component parameters at varying temperatures. Temperatures were swept through the range of -35 °C to +40 °C, to match the conditions in time-series temperature data utilized for computing total system performance.

In the case of variable fan speed, the simulation optimized the total system output by iteratively searching for the optimum fan speed for each temperature. It is important to note that optimization was based upon *net system output,* not efficiency. For a fixed system, the solution that maximizes output from the given system at the imposed ambient temperature will not, in general, match the optimum efficiency at that temperature if component properties are variable.

Finally, to better measure the performance of the simulated system, hourly temperature data from SRRL was used to simulate three years of operation, 2008-2010. A histogram summarizing the frequency at which each temperature occurred is shown in Figure 2.

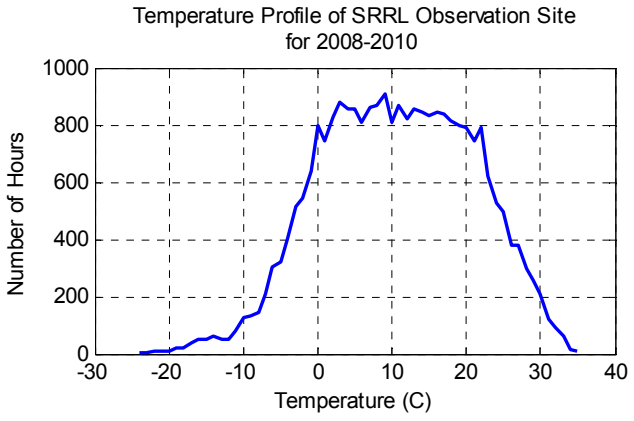

Figure 2: Histogram of Temperature Data

3. RESULTS

Results are presented in three sections. First, we consider the impact of variable fan speed without limiting the waste heat available. This configuration, while unrealistic, allows the simulation to operate at the optimum expander conditions for every temperature. Next, we consider the impact of fan speed on the realistic case of finite waste heat. Finally, we consider the impact of *fixed* versus *inf* expander types.

3.1 VARIABLE FAN SPEED, UNLIMITED WASTE HEAT

With the constraint on input heat removed, the optimum solution at each temperature is to maximize input heat to increase the net output of the system, as shown in Figure 3. By increasing fan speeds at low temperature to as high as 125% of nominal, the total mass flow is increased, significantly narrowing the exit temperature difference in the condenser (Figure 4) at low temperatures.

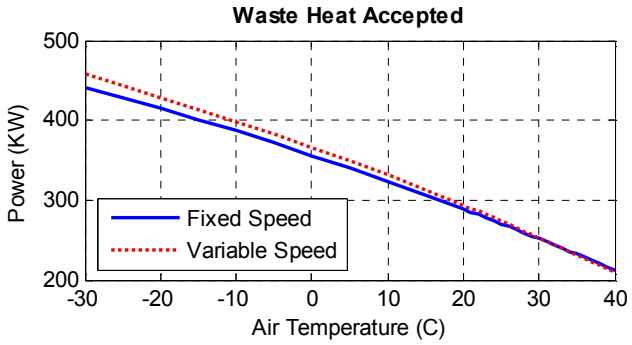

Figure 3: Waste Heat Accepted for Unlimited Waste Heat Conditions

While increasing fan speed with decreasing temperature improves performance, the overall impact on the system is quite small. Figure 5 shows fan power increases while expander output increases, albeit at a slightly lower rate. For the three year simulation period, the addition of variable speed fans produces a net improvement in system performance of less than 1%, and is unlikely to justify the additional cost of variable speed drives.

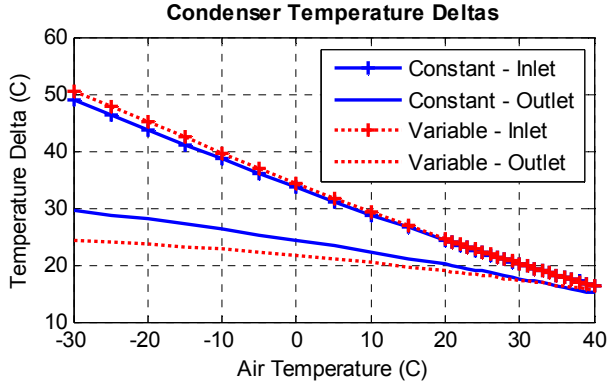

Figure 4: Condenser Temperature Deltas for Unlimited Waste Heat Conditions

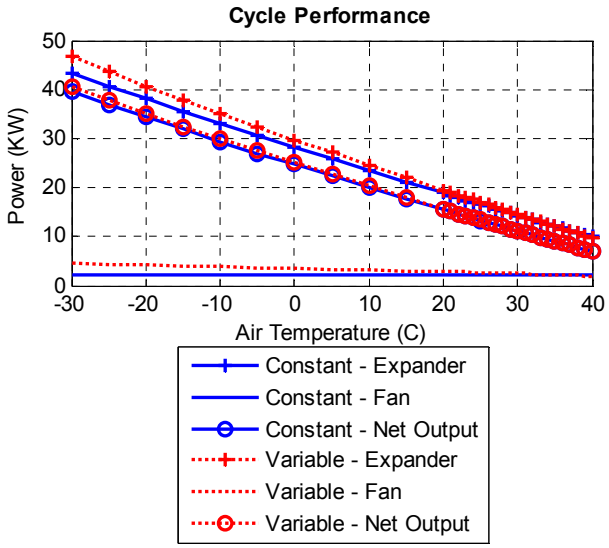

Figure 5: Cycle Performance for Unlimited Waste Heat Conditions

3.2 VARIABLE FAN SPEED, LIMITED WASTE HEAT

The study system was designed for operation at full waste heat input at 30 °C. Above that temperature, the pressure delta across the expander sets the flow rate. Below that temperature, boiler limitations effectively truncate Figure 3 at 250 KW of input power. Since waste heat temperatures at the boiler are constant, heat input to the ORC cycle can only be controlled by curtailing the mass flow rate with the turbine control valve, as shown in Figure 6. For fixed fan speeds, mass flow is curtailed below the design temperature by the control valve and above by the expander nozzles. However, in the case of variable speed fans, the optimum fan speed follows a complex trajectory over changing air temperature, with three distinct control regions. Figure 7 compares fan speed for limited and unlimited waste heat. At cold temperatures, the optimum speed is below design speed, raising the condenser temperature (Figure 8) and reducing the total pressure delta between the boiler and condenser. This change allows less pressure change to be taken in the control valve, as shown in Figure 9, increasing net system output. In effect, reducing fan power is more productive than increasing internal cycle efficiency.

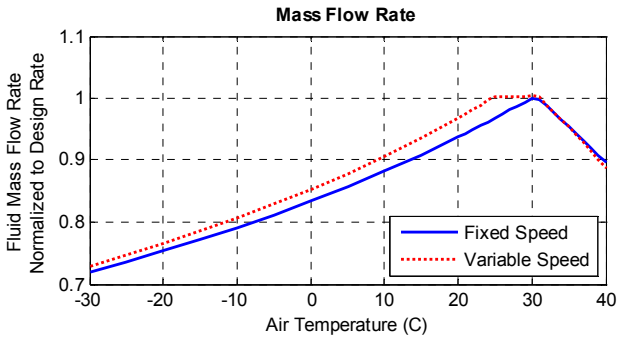

Figure 6: Fluid Mass Flow Rate for Limited Waste Heat Conditions

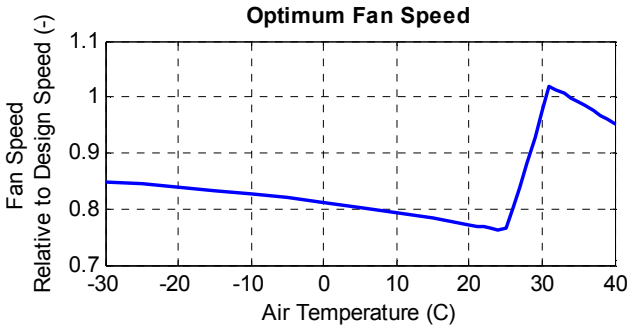

Figure 7: Optimum Fan Speed for Limited Waste Heat Conditions

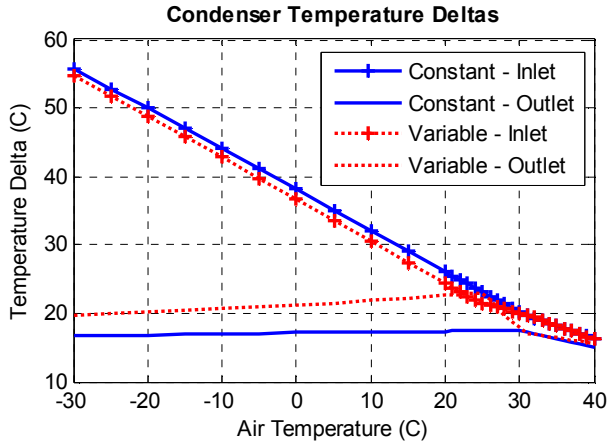

Figure 8: Condenser Temperature Deltas for Limited Waste Heat Conditions

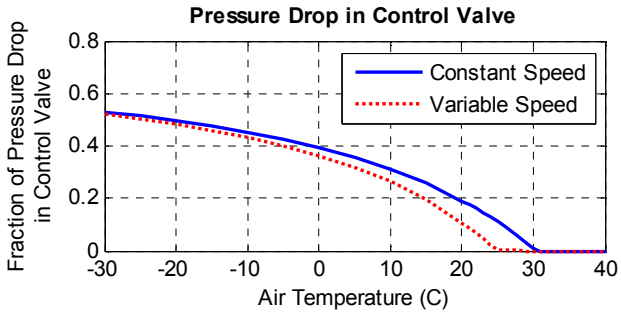

Figure 9: Fraction of Pressure Drop Taken in the Control Valve for Limited Waste Heat Conditions

However, below, but close to the design conditions, the optimum solution is to increase the fan speed, maximizing the pressure drop across the expander. Above the design conditions, the expander governs the mass flow rate, and little difference exists between any of the solutions.

For the three year simulation period, the addition of variable speed fans to the system increases total output by 3%, or ≅ 3.7 MWh/year. At an electricity price of $0.06/KWh this represents additional annual revenue ≅$220/year.

3.3 EXPANDER TYPE COMPARISON

Figure 10 compares overall cycle performance for both fixed-nozzle and infinitely-variable expanders. Unlike the introduction of variable-speed fans, an expander with independently controllable expansion ratio and mass flow rate has a significant impact on the cycle performance. Interestingly, changing to an *inf* expander significantly changes the optimum fan control protocol, as shown in Figure 11. The reason behind this change is clearly seen in Figure 12 – the *inf* expander produces better cycle efficiencies by maximizing temperature and pressure deltas at temperatures below the design conditions. Maximizing cycle efficiency in this case is more productive than minimizing fan loads – the opposite of the fixed-expander situation.

Considering the three-year study period, shifting from fixed to inf expander improves performance by ≅16.8% (≅$1270/year @ $0.06/KWh) with fixed-speed fans, or ≅19.5% (≅$1440/year @ $0.06/KWh) with variable-speed fans. These improvements could justify significant investment in controllable expansion-ratio expander devices.

Finally, it is interesting to note that for the *inf* expander case, the addition of variable speed fans has a larger impact than for the fixed-nozzle expander, improving the performance by nearly 6%.

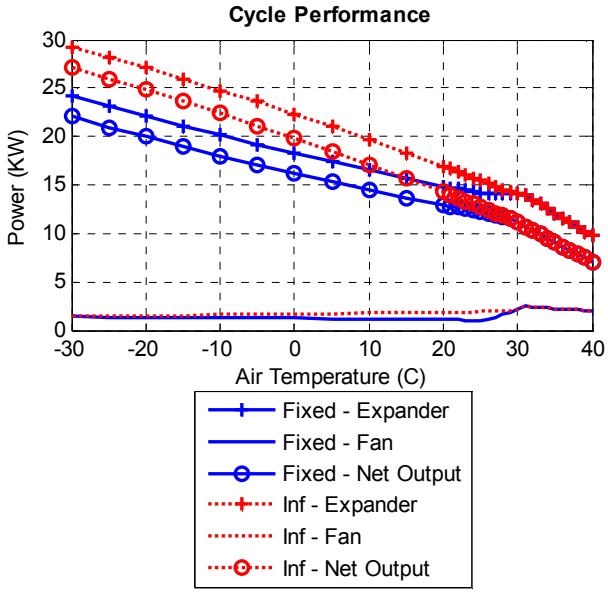

Figure 10: Cycle Performance for Fixed- and Infinitely-Variable Expanders with Variable-Speed Fans

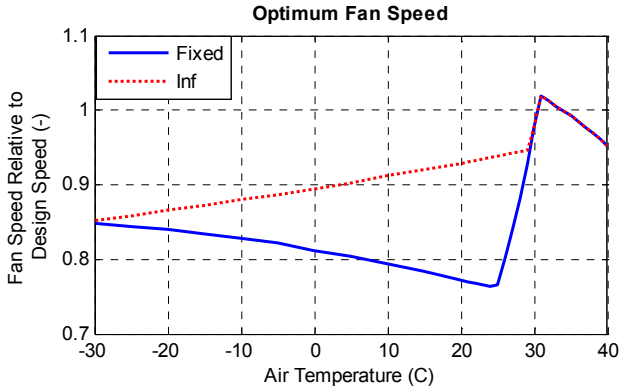

Figure 11: Optimum Fan Speed for Fixed- and Infinitely-Variable Expanders

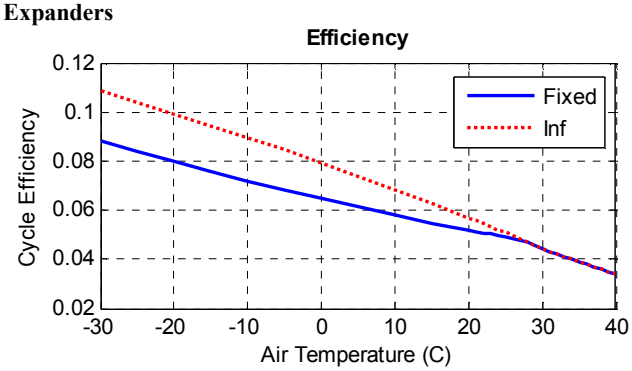

Figure 12: Cycle Efficiency for Fixed- and Infinitely-Variable Expanders

4. CONCLUSIONS

For most small waste-heat systems, expander performance remains a key challenge. Few practical variable-geometry or variable-expansion-ratio devices exist, and multi-stage devices are virtually non-existent below the multi-megawatt size. The current analysis clearly indicates that development of such devices could have significant positive impact on ORC waste heat solutions.

In contrast, the addition of variable-speed fans to systems with current fixed-geometry expanders represents a marginal proposition, producing relatively low improvements in overall power production.

The current analysis has several simplifications that deserve additional attention. These include improving the condenser model to more fully account for changes in heat exchange properties across differing fluid conditions and establishing more complete performance maps for both expander types. Future work could include a survey of additional working fluids and a similar analysis of higher-temperature waste heat sources.

5. REFERENCES

[1] Bailey O., and Worrell E., 2005, "Clean Energy Technologies: A Preliminary Inventory of the Potential for Electricity Generation."

[2] Madhawa Hettiarachchi H. D., Golubovic M., Worek W. M., and Ikegami Y., 2007, "Optimum design criteria for an Organic Rankine cycle using low-temperature geothermal heat sources," Energy, **32**(9), pp. 1698-1706.

[3] Heard C. L., Fernández H., and Holland F. A., 1990, "Development in geothermal energy in mexico--part twenty seven: The potential for geothermal organic rankine cycle power plants in Mexico," Heat Recovery Systems and CHP, **10**(2), pp. 79-86.

[4] Hung T. C., Wang S. K., Kuo C. H., Pei B. S., and Tsai K. F., "A study of organic working fluids on system efficiency of an ORC using low-grade energy sources," Energy, **In Press, Corrected Proof**.

[5] Astolfi M., Xodo L., Romano M. C., and Macchi E., "Technical and economical analysis of a solar-geothermal hybrid plant based on an Organic Rankine Cycle," Geothermics, **In Press, Corrected Proof**.

[6] Srinivasan K. K., Mago P. J., and Krishnan S. R., 2010, "Analysis of exhaust waste heat recovery from a dual fuel low temperature combustion engine using an Organic Rankine Cycle," Energy, **35**(6), pp. 2387-2399.

[7] Sternlicht B., 1982, "Waste energy recovery: An excellent investment opportunity," Energy Conversion and Management, **22**(4), pp. 361-373.

[8] Badr O., O'Callaghan P. W., and Probert S. D., 1990, "Rankine-cycle systems for harnessing power from low-grade energy sources," Applied Energy, **36**(4), pp. 263-292.

[9] "U.S. Environmental Protection Agency," http://www.epa.gov/highgwp1/scientific.html.

[10] Johnson K. M., Testimony on the U.S. Department of Energy's (DOE's) programs for developing water-efficient environmentally-sustainable energy-related technologies.

[11] DiPippo R., 2004, "Second Law assessment of binary plants generating power from low-temperature geothermal fluids," Geothermics, **33**(5), pp. 565-586.

[12] Bai O., Nakamura M., Ikegami Y., and Uehara H., 2004, "A Simulation Model for Hot Spring Thermal Energy Conversion Plant With Working Fluid of Binary Mixtures," J. Eng. Gas Turbines Power, **126**(3), pp. 445-454.

[13] Invernizzi C., Iora P., and Silva P., 2007, "Bottoming micro-Rankine cycles for micro-gas turbines," Applied Thermal Engineering, **27**(1), pp. 100-110.

[14] Yamamoto T., Furuhata T., Arai N., and Mori K., 2001, "Design and testing of the Organic Rankine Cycle," Energy, **26**(3), pp. 239-251.

[15] Nowak W., Borsukiewicz-Gozdur A., and Stachel A. A., 2008, "Using the low-temperature Clausius-Rankine cycle to cool technical equipment," Applied Energy, **85**(7), pp. 582-588.

[16] Zhang H., Wang E., Ouyang M., and Fan,Boyuan, 2011, "Study of Parameters Optimization of Organic Rankine Cycle (ORC) for Engine Waste Heat Recovery.pdf," Advanced Material Research, **201-203**, pp. 585-589.

[17] Gu W., Weng Y., and Cao G., 2007, "Testing and Thermodynamic Analysis of Low-Grade Heat Power Generation System Using Organic Rankine Cycle," K. Cen, Y. Chi, and F. Wang, eds., Springer Berlin Heidelberg, Hangzhou, China, pp. 93-98.
[18] Gu W., Weng Y., Wang Y., and Zheng B., 2009, "Theoretical and experimental investigation of an organic Rankine cycle for a waste heat recovery system," Proceedings of the Institution of Mechanical Engineers, Part A: Journal of Power and Energy, **223**(5), pp. 523-533.
[19] Lemmon E. W., Huber M. L., and McLinden M. O., REFPROP, NIST.